2018 17th IEEE International Conference on Machine Learning and Applications

Development of a Deep-Learning-Based Method for Breast Ultrasound Image Segmentation

Rania Almajalid[1,2], Juan Shan[1,*], Yaodong Du[1], Ming Zhang[3,4,*]
[1] Department of Computer Science, Seidenberg School of CSIS, Pace University, New York City, NY, USA
[2] College of Computing and Informatics, Saudi Electronic University, Riyadh, Saudi Arabia
[3] Division of Rheumatology, Tufts Medical Center, Boston, MA, USA
[4] Computer Science and Networking, Wentworth Insitute of Technology, Boston, MA, USA
ra56319p@pace.edu, jshan@pace.edu, yd67578n@pace.edu, MZhang@tuftsmedicalcenter.org

***Abstract*— Breast cancer is one of the deadliest cancers that cause women death globally. Ultrasound imaging is one of the commonly used diagnostic tools for detection and classification of breast abnormalities. In the past decades, computer-aided diagnosis (CAD) systems have been developed to improve the accuracy of diagnosis made by radiologists. In particular, automatic breast ultrasound (BUS) image segmentation is a critical step for cancer diagnosis using CAD. However, accurate tumor segmentation is still a challenge as a result of various ultrasound artifacts. This paper developed a novel segmentation framework based on deep learning architecture u-net, for breast ultrasound imaging. U-net is a convolutional neural network architecture designed for biology image segmentation with limited training data. It was originally proposed for neuronal structure segmentation in microscopy images. In our work, we modified and improved the method for BUS image segmentation. On a database of 221 BUS images, we first applied pre-processing techniques including contrast enhancement and speckle reduction to improve the image quality. Then the u-net model was trained and tested through two-fold cross-validation. In order to increase the size of training set, data augmentation strategies including rotation and elastic deformation were applied. Finally, a post-processing step that removed noisy region(s) from the segmentation result finalized the whole method. The area error metrics, dice coefficient, and similarity rate were calculated to evaluate the performance on the testing sets. We compared our method with another two fully automatic segmentation methods on the same dataset. Our method outperformed the other two significantly with the dice coefficient = 0.825 and similarity rate = 0.698. Experiment results showed that the modified u-net method is more robust and accurate in breast tumor segmentation for ultrasound images.**

Keywords*— *breast cancer; ultrasound images; automatic tumor segmentation; deep learning; u-net; convolutional neural networks; computer-aided diagnosis.

I. INTRODUCTION

Breast cancer is the most registered cancer among women, and it is known to be one of the deadliest cancers that cause the highest number of deaths globally [1]. It is still unclear to scientists what is exactly the cause of breast cancer. Early detection of the symptoms and signs is the primary way to reduce deaths resulting from breast cancer. Breast ultrasound (BUS) imaging coupled with the computer-aided diagnosis (CAD) system has turned out to be one of the most efficient and effective methodologies for the detection of cancer because of its painless, cost-effective, non-invasive, and non-radioactive nature [2].

Computer-aided diagnosis (CAD) systems for B-mode breast ultrasound have the ability to overcome intra- and inter-variability that is associated with the diagnosis of breast cancer, and clinical tests have indicated that they are at a position to improve diagnosis accuracy of breast cancer [3, 4]. Automatic BUS segmentation, which outlines the tumor region from the rest of the tissue regions on a BUS image, is a critical step for a CAD system. It has the ability to transform the conventional subjective tumor evaluation into accurate and reproducible tumor region measurements that are operator independent. As a result of clinical demands, as well as its challenging nature, automated BUS image segmentation research has been a center of attention within the past two decades. The existing approaches can be classified into fully automated or semi-automated methods based on whether user interactions are required. In semi-automatic approaches, the radiologist needs to specify the region of interest (ROI), which may include the lesion, an initial boundary, or a seed point in the lesion [11, 22]. On the other hand, fully automatic segmentation methods do not require the intervention of users, and they normally model the breast oncology and ultrasound knowledge as the preceding constraints [20, 21]. However, the automation is usually obtained with the sacrifice of accuracy and robustness of the methods. Achieving fully automatic segmentation with satisfactory accuracy is still a challenging and demanding task.

Deep learning (DL) methods, which are well known for their capability to extract high level features, have effectively addressed some of the critical problems in audio and vision fields [5, 6, 7]. DL methods have the ability to directly learn from the raw input, extract complex higher level attributes layer by layer, and finally lead to excellent performance of classification and segmentation. In the recent past, the interest in the application of DL approaches for medical image processing has been on the rise [8]. U-net [9] is a DL method that has a specially designed U-shaped convolutional network architecture. U-net was originally proposed for neuronal structure segmentation in microscopy images, and it won the ISBI challenge because of the precise and fast segmentation result. Since u-net is good at handling situations with small

* Corresponding Authors: Juan Shan, jshan@pace.edu and Ming Zhang, MZhang@tuftsmedicalcenter.org

978-1-5386-6805-4/18/$31.00 ©2018 IEEE
DOI 10.1109/ICMLA.2018.00179

training datasets, its excellent performance on microscopy images inspired us to apply it for BUS image segmentation. For the past two decades, many of the BUS studies have achieved excellent performances by utilizing their own private datasets and different quantitative metrics, which makes effective and objective comparisons among the approaches difficult.

In this paper, we developed a fully automatic segmentation framework for breast tumors using u-net as its core. To the best of our knowledge, this is the first time that u-net has been utilized to solve a BUS image segmentation issue. It should be noted that this method totally overrides the need to specify the region of interest (ROI), initial boundary, or a seed point in the lesion. U-net directly learned from the input images and corresponding image segmentation ground truths. At the same time, there is no requirement to tune any parameter for a dataset as the method can be self-adjusted when applied on a difference dataset.

The rest of the paper is organized as follows. A discussion of each step of this work is presented in section II, including pre-processing, the detailed structure of u-net, training/testing, and post-processing. The experimental setup procedure is reviewed in section III. Section IV reports and analyzes the experiment results and conclusion is drawn in section V.

II. Method

A. Speckle Reduction

Speckle is defined as a multiplicative noise that is locally correlated, which plagues imaging quality and affects medical image analysis. Speckle reduction methods are used to eliminate the speckle noise without tampering with the features of the image. In this work, we employed the commonly used Speckle Reducing Anisotropic Diffusion (SRAD) method [10], which is tailored for ultrasonic and radar imaging applications.

B. Contrast Enhancement

In this work, histogram equalization has been used to increase contrast. Fig. 1 provides an example of applying histogram equalization to an image in the database. After histogram equalization, the contrast between the tumor and surrounding tissues became stronger, and the intensity values were distributed more evenly throughout the whole intensity range [0, 255].

C. Deep Convolutional Networks

Convolutional neural network (CNN) [14], is defined as deep learning architecture that requires minimal preprocessing and directly extracts features from image pixels. The latest research in computer vision as well as pattern recognition has indicated that the CNNs have the capability to solve exigent tasks including object detection, segmentation, and classification, exhibiting state-of-the art performances, CNNs have been outstanding in various visual recognition undertakings including [12, 13]. CNNs are made up of subsampling and convolutional layers and have the ability to identify patterns that cannot be presented by hand-crafted features. Once a CNN is provided with enough labeled data, it is able to produce an excellent hierarchical representation of the raw input images. However, when CNNs are applied to solve medical image problems, the shortage of enough labeled

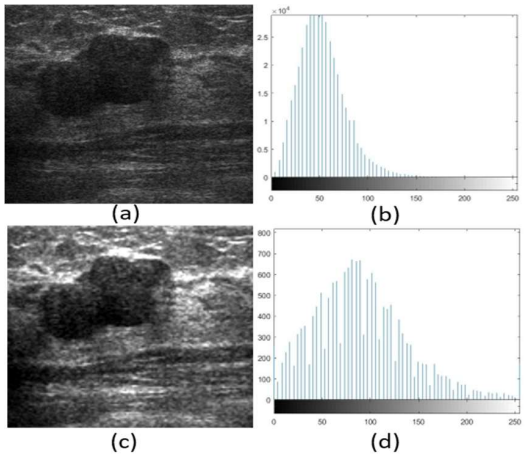

Fig. 1 (a)-(b) Original image from dataset and its corresponding histogram. (c)-(d) Resultant image after contrast enhancement and its corresponding histogram.

medical images is always an impediment for training a good model.

D. U-net

U-net [9] is a convolutional network architecture designed for precise and fast segmentation of images. The u-net's architecture consists of an expansive path on the right side and a contracting path on the left side as illustrated in [9] (see Fig. 2). The contracting path on the left follows a typical convolution network architecture. It is made up of two 3x3 convolution layers. Each layer is reinforced by a 2x2 max pooling operation that has stride 2 which is used for down-sampling. As well, each layer is followed by a rectified linear unit (ReLU). The expansive path on the right is made up of the following components. (1) An up-sampling of the feature maps. (2) 2x2 convolution layers which reduce the number of feature channels into half that is considered as a concatenation part. The feature map of the concatenation part is correspondingly cropped from the contracting path. (3) Two 3x3 convolution layers. (4) Each layer is reinforced by a ReLU function.

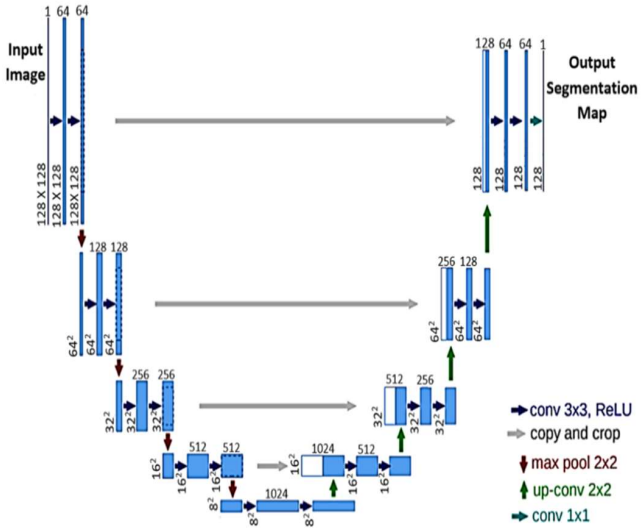

Fig. 2 U-net architecture [9].

In the final layer, mapping of the 64-dimensional feature vectors to the pre-defined number of classes is done using a 1x1 convolution layer. The network has 31,030,593 parameters which need to be trained, and it is made up of 23 convolutional layers.

The contraction phase increases the contextual information that defines an object's nature, and also reduces the spatial dimension. On the other hand, the expansion phase is attributed to the recovery of object details and dimensions. Further, concatenating feature maps from the contraction phase aid the expansion feature to recover the information about the location of the respective object. Also, they help to acquire the general information that combines the context and the localization. Such information is essential for the generation of an accurate segmentation map. U-net is considered as an end-to-end pipeline that is able to preserve the full context of the input images. U-net is able to process the entire image and produce the segmentation map at the same time in the forward pass.

E. Post-processing

A post-processing step was used to remove noisy region(s) from the u-net output. We noticed that for some cases u-net detected not only the tumor region, but also some false positive regions, such as the shadows (see Fig. 3). However, those false positive regions were all smaller than the true tumor region, so we could easily remove them by keeping only the largest region in an output image. This is based on the assumption that each image contains one tumor, which is true for our dataset. Fig. 5 illustrates an example of the post-processing step that removes noisy region(s).

III. Experimental Setup

A. Dataset

The dataset contains 221 BUS images. The images were collected by the doctors from the Second Affiliated Hospital of Harbin Medical University in China using a VIVID 7 (GE, Horten, Norway) with a linear probe of 5-14 MHz. Each image has a corresponding binary mask as the ground truth of the segmentation, which was generated from the manual delineation of the tumor by an experienced radiologist.

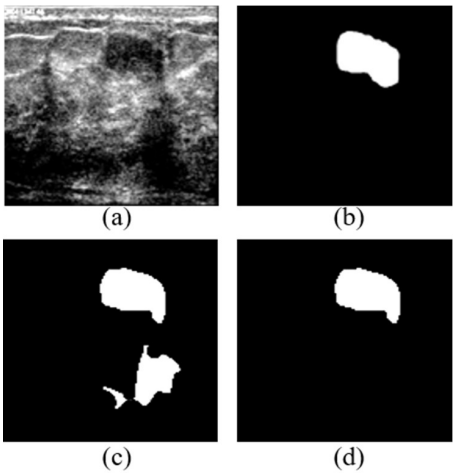

Fig.3. (a) Raw Image. (b) Ground truth mask. (c) Output from u-net. (d) Result after post-processing.

B. Data Augmentation

Deep neural networks often require a large amount of training data in order to achieve satisfactory performance. When it comes to medical imaging related tasks, the number of available medical images is always limited; therefore, data augmentation becomes a commonly used method to increase the size of medical image dataset. Different augmentation strategies were utilized in previous work, such as rotation, random crop, contrast change, etc. In this work, we utilized the rotation by 90 degree each time and elastic deformation. Be noted that augmentation was only done for the training dataset and the testing dataset was not touched.

The elastic deformation was performed by defining a normalized random displacement in the image space [23]. In the scope of unsupervised feature learning, Dosovitskiy et al. [15] depicted the essence of data augmentation when it comes to learning invariance. Elastic deformations enable the network to learn the invariance of the boundary between foreground and background, under different deformations situations. This strategy is useful for generating more close-to-real biomedical images for segmentation task because natural deformation is viewed as the most frequent variation in tissue, and realistic deformations can be easily and efficiently simulated. In this work, OpenCV library [16] was used to carry out image deformation. Geometrical transformations associated with 2D images are carried out by the *getAffineTransform* function contained in the OpenCV library. It does not tamper with the content of the image, but deforms the pixel grid and maps it into the destined image. The parameter that controls the extent of deformation was set between 0.08~1.0 to obtain different deformation effect. In a bid to avoid sampling artifacts, the mapping process began from the destination to the source and not vice versa. For each original image in the training set, three more deformed images were generated. Fig. 4 shows an example of image deformation.

Besides elastic deformation, rotation was also used to increase the size of the dataset. It is possible to preserve the dimensions of the image once rotated at right angles when the training images have a square shape. Each of the images are rotated at an angle of 90 degrees in the clockwise direction with respect to the initial one, which resulted in three new images additional to the original image. Fig. 5 depicts an example of image rotation.

C. Implementation

For convenience of image rotation and efficiency of network training, images and their corresponding masks were resized to 128 x 128 pixels. The dataset was then divided randomly into two groups, namely A and B, with each of the groups containing 50% of total images. Two-fold cross-validation was done by using group A as a training, and group B as a testing set for the first model; then the second model used group B for training and group A for testing. The average performance of the two models on the testing sets was reported and every sample was used as testing data once.

Keras [17] coupled with TensorFlow backend [18] in Python 3.5 was used to implement the u-net. A personal computer outfitted with a NVIDIA GoForse940MX graphics processing unit (GPU) was used to conduct all the experiments. The Adam

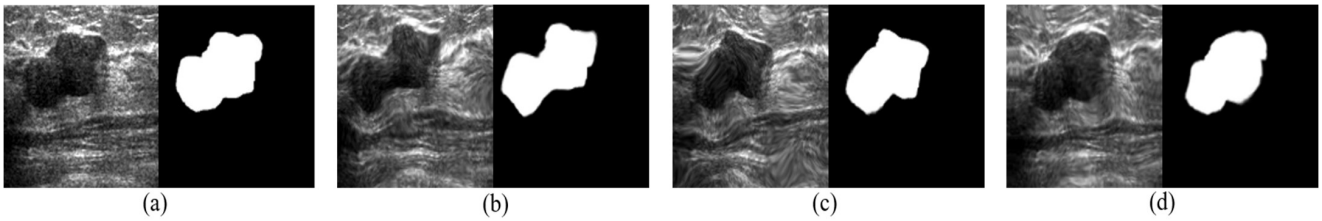

Fig. 4. (a) Original image and its mask. (b)–(d) Results after applying elastic deformation and their corresponding masks.

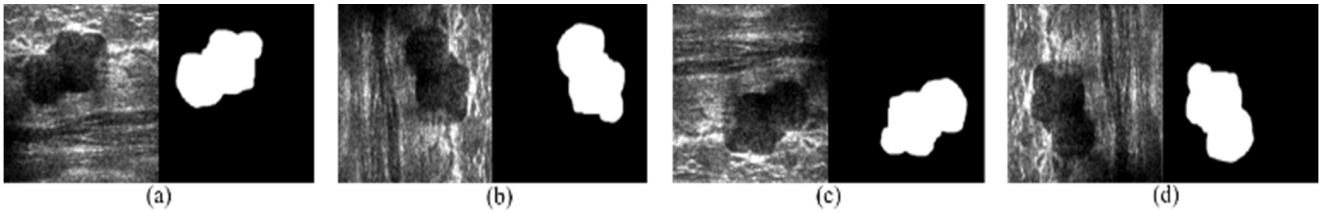

Fig. 5. (a) Original image and its mask. (b)–(d) Results after applying rotation and their corresponding masks.

Optimizer method was used to train the networks using the Dice Coefficient (DICE) as measure for accuracy of the segmentation procedure, whereas the minus DICE was used as a loss function which was back propagated through the CNN. The batch size was set to eight. Each of two the models were trained for 300 epochs, and the learning rate was initially set to 10^{-5}.

IV. Experiment Results

A. Evaluation Metrics

The most commonly used metric in validating medical image segmentation tasks is the dice coefficient (DICE) [19], which is also regarded as the overlap index. DICE is computed by directly comparing the ground truth and the automatic segmentation results, through the measure of spatial overlap rate between two binary images. The values range between 0 and 1, with 0 representing no overlap and 1 representing a perfect match. Equation (1) provides the Dice formula.

$$DICE = \frac{2*|A_m \cap Aa|}{|A_m| + |A_a|} \quad (1)$$

Besides DICE, we also computed area error metrics to evaluate segmentation accuracy from other perspectives. The true positive (TP) ratio, false positive (FP) ratio, false negative (FN) ratio, as well as the similarity (SI) can be calculated as following:

$$TP\ area\ ratio = \frac{|A_m \cap Aa|}{|A_m|} \quad (2)$$

$$FP\ area\ ratio = \frac{|A_m \cup Aa - A_m|}{|A_m|} \quad (3)$$

$$FN\ area\ ratio = 1 - TP\ area\ ratio \quad (4)$$

$$SI = \frac{|A_m \cap Aa|}{|A_m \cup A_a|} \quad (5)$$

The A_m refers to the pixel set of the lesion region outlined manually by the radiologist, whereas A_a refers to the lesion region automatically generated by the u-net model. Fig. 6 is an illustration of the area that corresponds to TP, FP, as well as FN. SI is an overall measure of the similarity between the two contours.

B. General Performance

In this study, we developed an u-net based fully automatic method for breast tumor segmentation. Different models were trained with different data augmentation strategies. Table I summarized the average performance of five models. The first model did not use any data augmentation strategy but the plain training set. The second model applied image rotation which increased the size of the training set four times more than the original set. The third model applied elastic deformation on the original set, generating four times more images, whereas in the fourth model, eight times more images were generated by deformation. The best performance was achieved by the fifth model where deformation was applied eight times then rotation was applied four times on the deformed images, thus amplifying the training set 32 times larger than the original set. Fig. 7 depicts three segmentation examples of the fifth model.

After 300 epochs, DICE of the fifth model reached 0.994 in the training set and 0.8252 in the testing set. Training and testing curves of DICE coefficient over epochs are provided in Fig. 8.

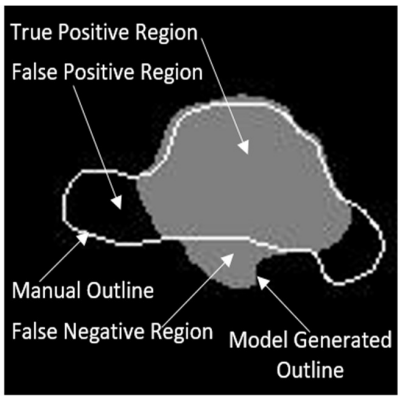

Fig. 6. Areas corresponding to TP, FP and FN regions.

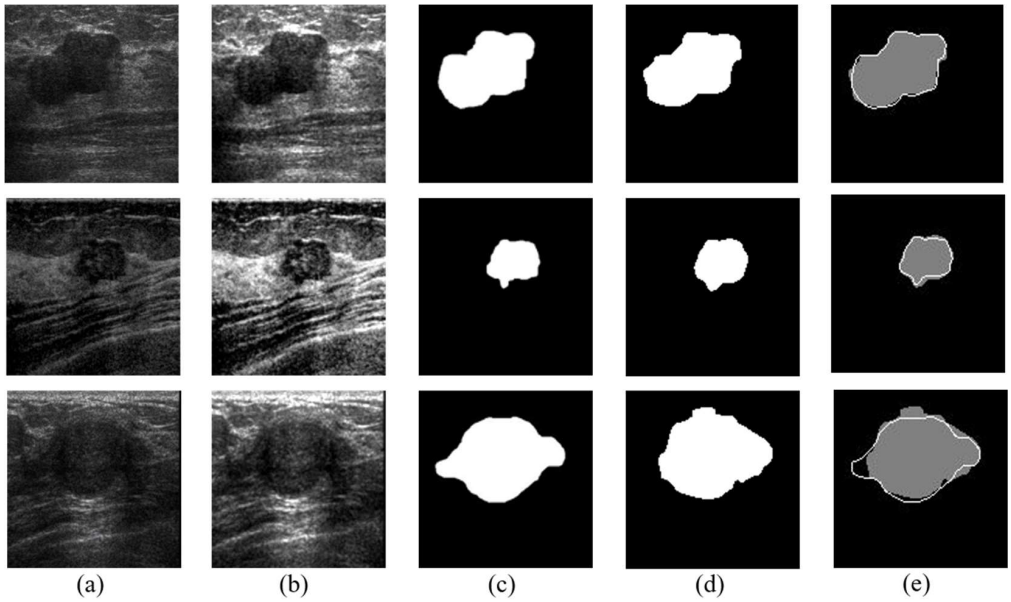

Fig. 7. (a) Raw Images. (b) Images after pre-processing. (c) Ground truth masks. (d) Output from u-net. (e) Overlap between the automatic segmentation and the ground truth annotation.

TABLE I. THE PERFORMANCE OF FIVE U-NET MODELS WITH DIFFERENT AUGMENTATION STRATEGIES

Model [a]	TP (%)	FP (%)	FN (%)	SI (%)	DICE (%)
1	69.57	25.10	30.43	60	75
2	78.45	30.02	21.55	65.85	79.67
3	75.46	19.97	24.54	64.08	78.54
4	77.28	27.43	22.72	65.62	79.86
5	78.66	18.59	21.34	69.76	82.52

[a.] Model 1 used no augmentation; model 2 used rotation; model 3 used deformation 4 times; model 4 used deformation 8 times; model 5 used 8 times deformation + rotation.

C. Comparison with Other BUS Segmentation Methods

Graph-based method is one of the BUS image segmentation approaches that are commonly used. The graph-based approaches have gained popularity due to their efficiency in the energy-optimization and its flexibility. The graph cuts and the Markov random field – Maximum a posteriori – Iterated conditional mode (MRF-MAP-ICM) are the two main frameworks in the graph-based methods. Xian et al. postulated a fully automated framework for BUS image segmentation whereby the graph cuts modeled the information derived from both the space domain and frequency domain [20]. The terminology, 'likelihood energy', modeled the position and pose of a tumor, as well as the distribution of the intensity.

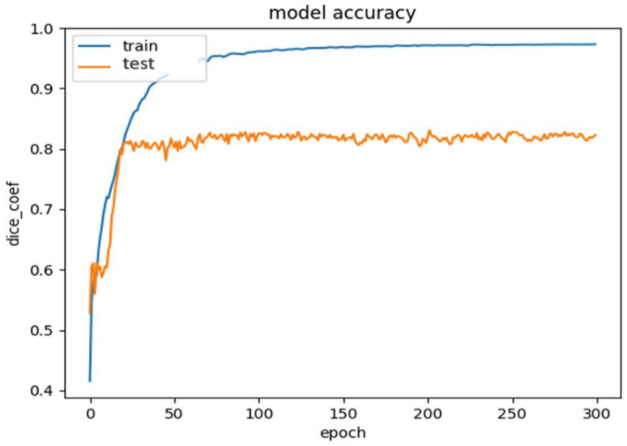

Fig. 8. Learning curves with DICE over epochs.

Learning-based methods are another major type of image segmentation methods. Both the unsupervised and supervised learning methods have been utilized to resolve BUS image segmentation problems. The unsupervised methods are fast, simple, and mostly used to generate candidate image regions as pre-processing. Supervised methods are excellent at the integration of features at various levels. Shan et al. [21] proposed a learning-based method which was an extension to the fuzzy c-means (FCM) clustering. The proposed neutrosophic l-means (NLM) clustering addressed the weak boundary predicament of the BUS image segmentation by taking into consideration the indeterminacy of membership.

We compared our method with the above two methods which are also fully automatic. The source code of both methods was obtained from the authors and the methods were evaluated on the same dataset. Table II summarized the performance of the two methods, as well as the performance of our fifth model. During our evaluation, all the parameters were adopted directly from the original papers.

As Table II shows, our method outperforms the other two methods in all the evaluation metrics significantly. The average DICE reached 82.52% and average similarity reached 69.76%. The method in [20] achieved better performance than that of the method in [21] in general, but both of these two methods had many failure cases on our dataset. We define a failure case as a case when no reasonable contour of the tumor is detected. For example: the detected tumor grows to the entire image, or the

TABLE II. PERFORMANCE COMPARISON WITH ANOTHER TWO METHODS

Method	TP (%)	FP (%)	FN (%)	SI (%)	DICE (%)
Xian et al. [20]	60.06	52.54	39.94	49.79	61.54
Shan et al. [21]	71.62	197.60	28.38	45.25	57.19
Our proposed method	78.66	18.59	21.34	69.76	82.52

detected contour includes a large area of non-tumor region, such as shadows. We noticed the performance of the two methods was much lower than that was reported in the original papers. This could be caused by using a different dataset; our dataset is larger and contains more difficult cases. Another reason could be that these two methods are highly dependent on parameter tuning, while we did not do any tuning but used their original parameters obtained on their own datasets. Through the comparison, u-net has shown its strong ability in detecting and segmenting true lesion boundaries in breast ultrasound images, as well as its superiority on self-learning and adjusting without any manual parameter tuning requirement.

V. CONCLUSION

This study has developed a u-net based segmentation framework for breast tumors using ultrasound images. With pre-processing, data augmentation, u-net training, and post-processing steps, an end-to-end fully automatic tumor segmentation pipeline was developed. Using two-fold cross-validation on a BUS dataset of 221 images, the method achieved 82.52% in term of average DICE. The method was compared with two state-of-the-art BUS segmentation approaches which were fully automatic too. Our method outperformed both of these two methods significantly on the same dataset with 221 images. The experiment results demonstrated that u-net architecture can be successfully applied to breast ultrasound image segmentation problems with robust and improved performance.

One of our future works is to investigate the current failure cases with an attempt to customize the method to fix these cases. These failure cases were counted into the current evaluation but solving them will further improve the performance of the method. Additionally, we plan to evaluate our method on new datasets. Another direction is to apply the u-net based framework to other medical imaging problems, such as segmentation for 3D MRI or CT.

ACKNOWLEDGMENT

This research is supported by National Institutes of Health awards (NIH-R01AR057802, NIH-U01AR067168), National Science Foundation awards (NSF-1723429, NSF-1723420), and Rheumatology Research Foundation award.

REFERENCES

[1] R. L. Siegel, K. D. Miller, and A. Jemal, "Cancer statistics, 2015,"CA:a cancer journal for clinicians, vol. 65, no. 1, pp. 5–29, 2015.

[2] H.-D. Cheng, J. Shan, W. Ju, Y. Guo, and L. Zhang, "Automated breastcancer detection and classification using ultrasound images: A survey,"Pattern recognition, vol. 43, no. 1, pp. 299–317, 2010.

[3] Y. Jiang, R. M. Nishikawa, R. A. Schmidt, C. E. Metz, M. L. Giger,and K. Doi, "Improving breast cancer diagnosis with computer-aideddiagnosis,"Academic radiology, vol. 6, no. 1, pp. 22–33, 1999.

[4] C. M. Sehgal, S. P. Weinstein, P. H. Arger, and E. F. Conant, "A review of breast ultrasound,"Journal of mammary gland biology and neoplasia,vol. 11, no. 2, pp. 113–123, 2006.

[5] H. Lee, R. Grosse, R. Ranganath, and A. Y. Ng, "Convolutional deepbelief networks for scalable unsupervised learning of hierarchical repre-sentations," inProceedings of the 26th annual international conferenceon machine learning, pp. 609–616, ACM, 2009.

[6] H. Lee, P. Pham, Y. Largman, and A. Y. Ng, "Unsupervised feature learning for audio classification using convolutional deep belief networks,"inAdvances in neural information processing systems, pp. 1096–1104,2009.

[7] Q. V. Le, W. Y. Zou, S. Y. Yeung, and A. Y. Ng, "Learning hierarchicalinvariant spatio-temporal features for action recognition with indepen-dent subspace analysis," inComputer Vision and Pattern Recognition(CVPR), 2011 IEEE Conference on, pp. 3361–3368, IEEE, 2011.

[8] A. A. Cruz-Roa, J. E. A. Ovalle, A. Madabhushi, and F. A. G.Osorio, "A deep learning architecture for image representation, visualinterpretability and automated basal-cell carcinoma cancer detection," inInternational Conference on Medical Image Computing and Computer-Assisted Intervention, pp. 403–410, Springer, 2013.

[9] O. Ronneberger, P. Fischer, and T. Brox, "U-net: Convolutional networksfor biomedical image segmentation," inInternational Conference onMedical image computing and computer-assisted intervention, pp. 234–241, Springer, 2015.

[10] Y. Yu and S. T. Acton, "Speckle reducing anisotropic diffusion,"IEEETransactions on image processing, vol. 11, no. 11, pp. 1260–1270, 2002.

[11] Z. Zhou, W. Wu, S. Wu, P.-H. Tsui, C.-C. Lin, L. Zhang, and T. Wang,"Semi-automatic breast ultrasound image segmentation based on meanshift and graph cuts,"Ultrasonic imaging, vol. 36, no. 4, pp. 256–276,2014.

[12] R. Girshick, J. Donahue, T. Darrell, and J. Malik, "Rich featurehierarchies for accurate object detection and semantic segmentation,"inProceedings of the IEEE conference on computer vision and patternrecognition, pp. 580–587, 2014.

[13] A. Krizhevsky, I. Sutskever, and G. E. Hinton, "Imagenet classificationwith deep convolutional neural networks," inAdvances in neural infor-mation processing systems, pp. 1097–1105, 2012.

[14] Y. LeCun, L. Bottou, Y. Bengio, and P. Haffner, "Gradient-based learningapplied to document recognition,"Proceedings of the IEEE, vol. 86,no. 11, pp. 2278–2324, 1998.

[15] A. Dosovitskiy, J. T. Springenberg, M. Riedmiller, and T. Brox, "Dis-criminative unsupervised feature learning with convolutional neuralnetworks," inAdvances in Neural Information Processing Systems,pp. 766–774, 2014.

[16] G. Bradski and A. Kaehler, "Opencv,"Dr. Dobbs journal of softwaretools, 2000.

[17] F. Chollet, "Keras," https://github.com/fchollet/keras, 2015.

[18] M. Abadi, A. Agarwal, P. Barham, E. Brevdo, Z. Chen, C. Citro,G. Corrado, A. Davis, J. Dean, M. Devin,et al., "Tensorflow: Large-scale machine learning on heterogeneous distributed systems," 2016.

[19] L. R. Dice, "Measures of the amount of ecologic association betweenspecies,"Ecology, vol. 26, no. 3, pp. 297–302, 1945.

[20] M. Xian, Y. Zhang, and H. Cheng, "Fully automatic segmentation ofbreast ultrasound images based on breast characteristics in space andfrequency domains,"Pattern Recognition, vol. 48, no. 2, pp. 485–497,2015.

[21] J. Shan, H. Cheng, and Y. Wang, "A novel segmentation method forbreast ultrasound images based on neutrosophic l-means clustering,"Medical physics, vol. 39, no. 9, pp. 5669–5682, 2012.

[22] G. Pons, J. Martí, R. Martí, S. Ganau, and J. A. Noble, "Breast-lesion segmentation combining b-mode and elastography ultrasound,"Ultrasonic imaging, vol. 38, no. 3, pp. 209–224, 2016.

[23] W. Mio, A. Srivastava, and S. H. Joshi, "On shape of plane elastic curves," International Journal of Computer Vision, vol. 73, no. 3, pp. 307–324, 2007.